Journal of Solid State Chemistry **149,** 149–154 (2000)
Article ID jssc.1999.8513, available online at http://www.idealibrary.com on IDEAL®

Dimorphism of the Vanadium(V) Monophosphate $PbVO_2PO_4$: α-Layered and β-Tunnel Structures

M. M. Borel,* A. Leclaire,* J. Chardon,* M. Daturi,† and B. Raveau*

*Laboratoire CRISMAT, UMR 6508 Associée au CNRS, and †Laboratoire LCS, UMR 6506 Associée au CNRS, ISMRA et Université de Caen, 6 Boulevard du Maréchal Juin, 14050 Caen Cedex, France

Received June 15, 1999; in revised form September 13, 1999; accepted September 21, 1999

Two forms of V(V) monophosphate α- and β- $PbVO_2PO_4$ have been synthesized and grown as single crystals. The α form is isostructural with the Ba and Sr homologues previously described by Kang *et al.* The β form exhibits an original tridimensional (3D) framework ($a = 9.715(1)$, $b = 13.820(1)$, and $c = 10.999(1)$ Å). The latter crystallizes in the space group *Pnma* and consists of tritetrahedral P_2VO_{10} units and tripolyhedral units V_2PO_{14} ($2VO_6$ octahedra + $1PO_4$ tetrahedron) forming chains running along *b*. VPO_8 chains in which one PO_4 tetrahedron alternates with one VO_6 octahedron, running along *a* and forming $[V_2P_2O_{14}]_\infty$ layers are also observed. This 3D framework forms large tunnels running along *b* where the Pb^{2+} cations are located. The infrared study supports the structure description and gives a tentative correlation between framework units and vibrational behaviour. © 2000 Academic Press

INTRODUCTION

Among the numerous phosphates of transition elements which have been discovered these last years, curiously very few V(V) phosphates have been synthesized, despite the ability of this element to accomodate various coordinations, from octahedral to pyramidal or tetrahedral. Besides the oxides of the system V_2O_5–P_2O_5 extensively explored for the generation of new catalysts (1,2), the only phosphates of the systems *A*–V–P–O, where *A* is either a bivalent or a univalent cation and vandium is pentavalent, are the phases A_2VPO_6 with $A =$ Na, K (3), Li (4) and Ag (5), KV_2PO_8 (6), $Zn_3(V_{0.5}P_{1.5})O_8$ (7), $Pb_3(V_{2-x}P_{2x})O_8$ (8), $Cd_2(VP)O_7$ (9), and more recently the compounds $SrVO_2PO_4$ and $BaVO_2PO_4$ (10). Moreover, the latter could only be prepared by hydrothermal synthesis. This behavior is unexpected if one takes into consideration the great ability of V(V) to accomodate various frameworks and suggests that vanadium (V) phosphates should be carefully explored for a better understanding, varying the synthesis methods. Starting from the results obtained by Kang *et al.* (10) for $PbVO_2PO_4$, which was found to be isostructural to the Sr and Ba phases, we have revisited the synthesis and crystal growth of this compound using various methods. We report herein on the dimorphism of this V(V) monophosphate, showing a layered structure built up of VO_6 octahedra and PO_4 tetrahedra for the α form prepared by hydrothermal synthesis in agreement with previous results (10), and an original tunnel structure involving VO_6 octahedra and VO_4 and PO_4 tetrahedra for the β-form prepared by solid state reaction in air.

CHEMICAL SYNTHESIS AND CRYSTAL GROWTH

The synthesis of α-$PbVO_2PO_4$ was carried out by hydrothermal synthesis according to experimental conditions similar to those described by Kang *et al.* (10) for the Ba and Sr homologues. A mixture of V_2O_5 (99%), H_3PO_4 (85%), and $PbCO_3$ (99%) from Prolabo and water in the molar ratio 0.5/1/1/555 was heated in a 23-ml Teflon container placed in a steel autoclave for 4 days at 493 K before cooling at 4 K h^{-1} to room temperature. The yellow product was filtered off, washed with water, rinsed with ethanol, and air dried at room temperature. Some yellow single crystals were extracted from this resulting product. The EDS analysis of these crystals led to a Pb/V/P ratio of 1:1:1. The X-ray diffraction powder pattern of the yellow product (Fig. 1a) was indexed in a monoclinic cell in agreement with the single crystal study (Table 1), confirming its isotypism with the AVO_2PO_4 ($A =$ Ba and Sr) phosphates previously published by Kang *et al.* (10).

β-$PbVO_2PO_4$ was synthesized by a solid state reaction method, starting from an intimate mixture of $PbCO_3$, $H(NH_4)_2PO_4$, and NH_4VO_4, in stoichiometric proportions, first heated at 673 K for 2 h, then heated at 873 K for 12 h, and finally quenched at room temperature. The crystal growth of this second form was carried out using a second solid state reaction procedure: first, the stoichiometric mixture of $PbCO_3$, $H(NH_4)_2PO_4$, and NH_4VO_4 was heated at 673 K for 2 h in a platinum crucible to decompose the carbonate, the ammonium phosphate, and ammonium

0022-4596/00 $35.00

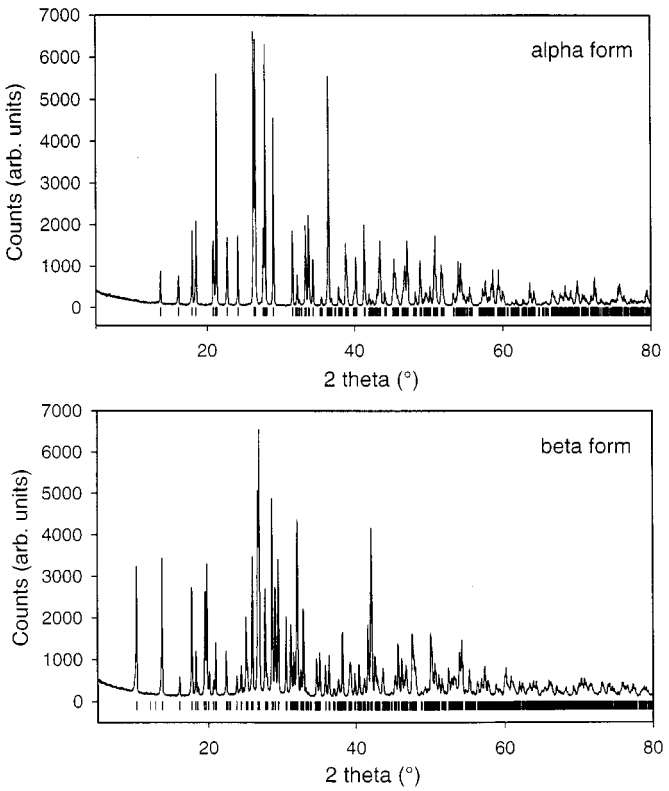

FIG. 1. XRPD patterns: (a) for α-$PbVO_2PO_4$; (b) for β-$PbVO_2PO_4$.

vanadate, and then in a second step the mixture was sealed in an evacuated silica ampoule, heated to 873 K for 48 h, and finally quenched to room temperature. Well-faceted yellow crystals were obtained for this new phase; their EDS analysis revealed the Pb:V:P molar ratio equal to 1:1:1, and their X-ray diffraction preliminary study showed an orthorhombic symmetry (Table 1). The XRPD pattern (Fig. 1b) of the sample prepared by the first solid state reaction procedure could be indexed in an orthorhombic cell deduced from the single-crystal study (Table 1), confirming its purity.

STRUCTURE DETERMINATION

Two crystals with dimensions $0.154 \times 0.102 \times 0.077$ and $0.179 \times 0.077 \times 0.077\ mm^3$ were selected for the structure determination respectively for the α and β forms of $PbVO_2PO_4$. The cell parameters initially measured on Weissenberg films and later refined by diffractometric techniques at 293 K with a least-square refinement based on 25 reflections are listed in Table 1. The systematic reflection conditions observed for α-$PbVO_2PO_4$, $l = 2n$ for $h0l$ and $k = 2n$ for $0k0$, are consistent with the $P2_1/c$ space group, confirming that it was isostructural with AVO_2PO_4 (A = Ba, Sr) (10). For β-$PbVO_2PO_4$ the reflection conditions $k + l = 2n$ for $0kl$ and $h = 2n$ for $hk0$ are consistent with the space groups *Pnma* and $Pn2_1a$. The data were collected on a CAD4 Enraf Nonius diffractometer with the parameters reported in Table 1. The reflections were corrected for Lorentz and polarization effects, for absorption (Gaussian method) and for secondary extinction. The structure of α-$PbVO_2PO_4$ was determined from the atomic parameters of the isostructural phosphate $SrVO_2PO_4$ (10) as a starting model. The refinement of the structure in the $P2_1/c$ space group allowed the agreement factors to be lowered to $R = 0.063$ and $R_w = 0.071$ for the atomic parameters listed in Table 2.

The structural determination of the β-$PbVO_2PO_4$ phosphate was performed by the heavy atom method and the refinement was successful in the *Pnam* centrosymmetric group, leading to $R = 0.041$ and $R_w = 0.040$ and to the atomic coordinates listed in Table 2.

DESCRIPTION OF THE STRUCTURES

α-$PbVO_2PO_4$ is isostructural with the two-layered V(V) monophosphates, $BaVO_2PO_4$ and $SrVO_2PO_4$, as previously stated by Kang *et al.* (10). The projection of the structure of this form along **c** (Fig. 2) shows indeed that it

TABLE 1
Summary of Crystal Data, Intensity Measurements, and Structure Refinement Parameters for $PbVO_2PO_4$ (α and β)

	α	β
	1. Crystal Data	
Space group	$P2_1/c$	*Pnma*
Cell dimensions	$a = 5.5016(4)$ Å	$a = 9.7150(8)$ Å
	$b = 9.8959(7)$ Å	$b = 13.820(1)$ Å
	$c = 8.5094(6)$ Å	$c = 10.9990(8)$ Å
	$\beta = 90.473(6)°$	
Volume (Å^3)	463.26(6)	1476.7(2)
Z	4	12
	2. Intensity Measurements	
λ(Mo$K\alpha$)	0.71073	0.71073
Scan mode	ω–θ	ω–θ
Scan width	$1.1 + 0.35 \tan\theta$	$1.1 + 0.35 \tan\theta$
Slit aperture (mm)	$1.1 + \tan\theta$	$1.1 + \tan\theta$
Max θ(°)	45	45
Standard reflections	3 measured every hour	
Reflections measured	4117	6695
Reflections with $I > 3\sigma$	2482	2399
μ (mm^{-1})	38.6	36.33
	3. Structure Solution and Refinement	
Parameters refined	83	134
Agreement factors	$R = 0.063$	$R = 0.041$
	$R_w = 0.071$	$R_w = 0.040$
Weighting scheme	$1/\sigma^2$	$1/\sigma^2$
Δ/σ max	0.002	0.001
$\Delta\sigma$ (eÅ^{-3})	13	3.45

TABLE 2
Atomic Positional and Isotropic Displacement Parameters

	x/a	y/b	z/c	U_{eq}
		For α-$PbVO_2PO_4$		
Pb	0.85790(8)	0.68225(4)	0.07190(5)	*0.01099(9)
V	0.3366(3)	0.5884(2)	0.4117(2)	*0.0058(3)
P	0.6626(5)	0.3889(3)	0.2146(3)	*0.0066(6)
O(1)	0.256(2)	0.6639(8)	0.621(1)	*0.011(2)
O(2)	0.519(2)	0.5246(8)	0.2266(9)	*0.010(2)
O(3)	0.499(2)	0.7804(8)	0.362(1)	*0.011(2)
O(4)	0.081(2)	0.6297(9)	0.331(1)	*0.013(2)
O(5)	0.692(1)	0.5709(8)	0.525(1)	*0.008(2)
O(6)	0.882(2)	0.4226(9)	0.115(1)	*0.014(2)
		For β-$PbVO_2PO_4$		
Pb(1)	0.8955(4)	0.10971(2)	0.61892(3)	*0.01167(7)
Pb(2)	0.46392(8)	$\frac{1}{4}$	0.51096(8)	*0.0347(2)
V(1)	0.2993(2)	0.5184(1)	0.4037(1)	*0.0078(3)
V(2)	0.1219(3)	$\frac{1}{4}$	0.3154(2)	*0.0148(6)
P(1)	0.1032(3)	0.4501(2)	0.1745(2)	*0.0075(5)
P(2)	0.2173(4)	$\frac{3}{4}$	0.2883(3)	*0.0074(8)
O(1)	0.3223(7)	0.4093(4)	0.4567(6)	*0.014(2)
O(2)	0.1296(7)	0.5324(5)	0.4493(7)	*0.015(2)
O(3)	0.3736(7)	0.5844(4)	0.5429(6)	*0.011(1)
O(4)	0.2389(7)	0.4853(5)	0.2301(6)	*0.012(2)
O(5)	0.4938(7)	0.5291(4)	0.3169(6)	*0.011(2)
O(6)	0.3000(7)	0.6613(4)	0.3293(6)	*0.013(2)
O(7)	0.071(1)	$\frac{1}{4}$	0.455(1)	*0.026(4)
O(8)	0.0512(8)	0.3599(4)	0.2458(7)	*0.017(2)
O(9)	0.287(1)	$\frac{1}{4}$	0.312(1)	*0.032(4)
O(10)	0.225(1)	$\frac{3}{4}$	0.1461(9)	*0.015(3)
O(11)	0.066(1)	$\frac{3}{4}$	0.326(1)	*0.018(3)

$U_{eq} = \frac{1}{3}\sum U_{ii}$

can be described as $[VPO_6]_\infty$ layers whose cohesion is ensured by Pb^{2+} cations. Each $[VPO_6]_\infty$ layer is built up from bioctahedral units interconnected with PO_4 tetrahedra, as shown from the projection of the structure along **a** (Fig. 3). Note that these polyhedra delimit eight-sided windows formed by four tetrahedra and four octahedra, which are aligned along **a**, so that the structure forms tunnels along this direction. The interatomic distances and angles (Tables 3a and 3b) are very similar to those observed for the Ba and Sr homologues (10). Like for these compounds, the PO_4 tetrahedra are slightly distorted with two longer P–O bonds (1.553 and 1.560 Å) and two shorter ones (1.532 and 1.526 Å). The VO_6 octahedra are strongly distorted with two abnormally short V–O bonds (1.609 and 1.673 Å), two intermediate distances (1.979 and 1.986 Å), and two abnormally long bonds (2.143 and 2.182 Å). The Pb^{2+} cations exhibit like Sr^{2+} and Ba^{2+} in AVO_2PO_4 (10) a 9-fold coordination with Pb–O distances ranging from 2.39 to 3.035 Å. The electrostatic valence sum calculated with the Brese and O'Keeffe (11) relation confirms the pentavalent character of vanadium and the divalent character of lead.

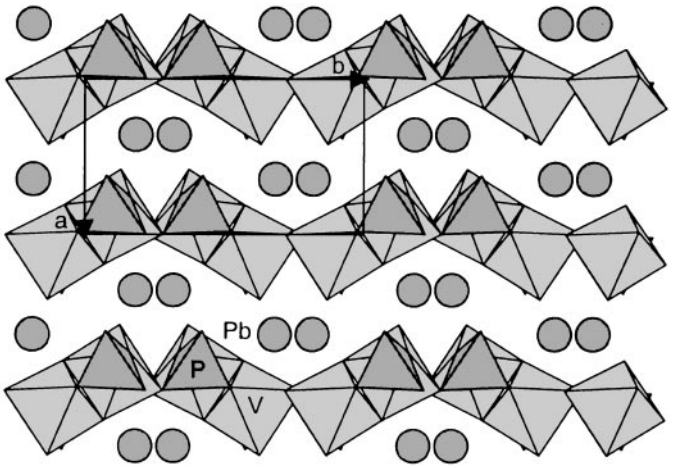

FIG. 2. Projection of the structure of α-$PbVO_2PO_4$ along **c**.

The structure of β-$PbVO_2PO_4$ is original. Its projection along **b** (Fig. 4) shows that the tridimensional $[VPO_6]_\infty$ framework consists of corner-sharing VO_6 octahedra, VO_4 tetrahedra, and PO_4 tetrahedra, forming large tunnels running along **b** where there are located the Pb^{2+} cations. The projection of the structure along **c** (Fig. 5) shows that the $[VPO_6]_\infty$ framework can be described by the assemblage of two sorts of tripolyhedral units ranging along **b**: tritetrahedral VP_2O_{10} units involving two P(1) tetrahedra and one V(2) tetrahedron and V_2PO_{14} units involving two V(1) octahedra and one P(2) tetrahedron. In those units each P(1) tetrahedron shares its four apices with three VO_6 octahedra and one VO_4 tetrahedron, whereas the P(2) tetrahedron

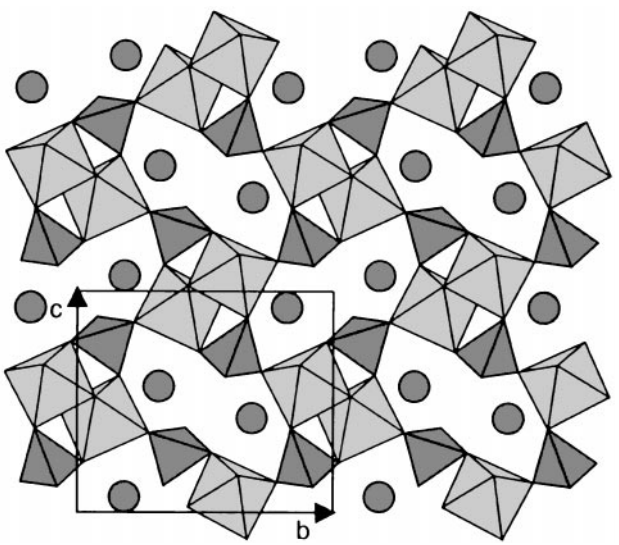

FIG. 3. Projection of the structure of α-$PbVO_2PO_4$ along **a**.

TABLE 3a
Distances (Å) and Angles (°) in the Polyhedra in the α-$PbVO_2PO_4$

V	O(1)	O(2)	O(3)	O(4)	O(5)	$O(5^{i})$
O(1)	1.986(9)	3.92(1)	2.84(1)	2.66(1)	2.70(1)	2.65(1)
O(2)	162.3(4)	1.979(9)	2.78(1)	2.78(1)	2.74(1)	2.60(1)
O(3)	86.7(4)	84.8(4)	2.143(9)	2.75(1)	2.71(1)	3.76(1)
O(4)	95.0(5)	100.9(4)	93.0(4)	1.609(9)	3.78(1)	2.64(1)
O(5)	80.6(4)	82.4(4)	77.7(4)	169.9(4)	2.182(9)	2.57(1)
$O(5^{i})$	92.6(4)	90.2(4)	160.0(4)	106.9(5)	82.5(4)	1.673(8)

P	$O(1^{i})$	O(2)	$O(3^{ii})$	O(6)
$O(1^{i})$	1.553(9)	2.58(1)	2.49(1)	2.52(1)
O(2)	111.8(5)	1.560(9)	2.53(1)	2.43(1)
$O(3^{ii})$	107.8(5)	109.9(5)	1.532(9)	2.53(1)
O(6)	110.5(5)	104.6(5)	112.3(5)	1.52(1)

$Pb–O(1^{iii}) = 2.699(9)$
$Pb–O(2) = 2.771(9)$
$Pb–O(3) = 2.318(9)$
$Pb–O(3^{iv}) = 2.682(9)$
$Pb–O4^{iii}) = 2.571(9)$
$Pb–O(4^{v}) = 3.035(9)$
$Pb–O(5^{iv}) = 2.636(8)$
$Pb–O(6) = 2.599(9)$
$Pb–O(6^{vi}) = 2.39(1)$

Symmetry codes

i:	$1-x$; $1-y$; $1-z$
ii:	$1-x$; $-0.5+y$; $0.5-z$
iii:	$1+x$; $1.5-y$; $-0.5+z$
iv:	x; $1.5-y$; $-0.5+z$
v:	$1+x$; y; z
vi:	$2-x$; $1-y$; $-z$

shares only two apices with two VO_6 octahedra, its two other apices being free. Each V(1) octahedron has two free apices, only being linked to four PO_4 tetrahedra, whereas each V(2) tetrahedron has also two free apices, only being linked to two PO_4 tetrahedra. In fact, this (001) projection (Fig. 5) allows two different types of layers parallel to (010) to be distinguished: mixed $[V_2P_2O_{14}]_\infty$ layers built up of corner-sharing V(1) octahedra and P(1) tetrahedra and pure tetrahedral layers $[VPO_8]_\infty$. The $[V_2P_2O_{14}]_\infty$ layers (Fig. 6a) are built up of corner-sharing V(1) octahedra and P(1) tetrahedra, forming $[VPO_8]_\infty$ zig–zag chains running along **a** and along **c**. In those chains, one V(1) octahedron alternates with one P(1) tetrahedron. Thus, these layers can be described either by the assemblage of [100] or of [001] $[VPO_8]_\infty$ chains. These chains form large windows delimited by four tetrahedra and four octahedra, where the Pb(1) cations are located. In the pure tetrahedral $[VPO_8]_\infty$ layers the V(2) tetrahedra and the P(2) tetrahedra are isolated (Fig. 6b), and Pb(2) cations are located at this level. Note that Pb(2) cations and P(2) and V(2) tetrahedra form rows running along **a**, which alternate according to the sequence "Pb(2)–P(2)–V(2)" along **c**. Finally, the $[VPO_6]_\infty$ tridimensional framework results from the association of two enantiomorphic $[V_2P_2O_{14}]_\infty$ layers which are interconnected through a tetrahedral $[VPO_8]_\infty$ layer.

TABLE 3b
Distances (Å) and Angles (°) in the Polyhedra in the β-$PbVO_2PO_4$

V(1)	O(1)	O(2)	O(3)	O(4)	O(5)	O(6)
O(1)	1.648(7)	2.531(7)	2.646(7)	2.823(7)	2.808(7)	3.760(7)
O(2)	100.6(3)	1.642(7)	2.682(7)	2.714(7)	3.827(7)	2.766(7)
O(3)	93.9(3)	95.8(3)	1.961(7)	3.928(7)	2.851(7)	2.675(7)
O(4)	100.0(3)	95.0(3)	160.5(3)	2.024(7)	2.722(7)	2.733(7)
O(5)	92.2(3)	166.9(3)	86.0(3)	79.9(3)	2.210(7)	2.628(7)
O(6)	166.0(3)	93.1(3)	81.3(3)	82.0(3)	74.4(3)	2.139(7)

V(2)	O(7)	O(8)	$O(8^{i})$	O(9)
O(7)	1.62(1)	2.77(1)	2.77(1)	2.63(1)
O(8)	106.4(4)	1.834(7)	3.04(1)	2.84(1)
$O(8^{i})$	106.4(4)	111.8(4)	1.834(7)	2.84(1)
O(9)	109.5(7)	111.3(4)	111.3(4)	1.61(1)

P(1)	$O(3^{ii})$	O(4)	$O(5^{iii})$	O(8)
$O(3^{ii})$	1.540(7)	2.522(9)	2.458(9)	2.471(9)
O(5)	110.3(4)	1.533(7)	2.510(9)	2.521(9)
$O(5^{iii})$	112.4(4)	110.3(4)	1.526(7)	2.501(9)
O(8)	105.9(4)	109.4(4)	108.4(4)	1.557(7)

P(2)	O(6)	$O(6^{iv})$	O(10)	O(11)
O(6)	1.533(7)	2.450(9)	2.47(1)	2.58(1)
$O(6^{iv})$	106.1(4)	1.533(7)	2.47(1)	2.58(1)
O(10)	105.8(4)	105.8(4)	1.57(1)	2.51(1)
O(11)	115.1(4)	115.1(4)	108.2(6)	1.53(1)

$Pb(1)–O(1^{i}) = 2.892(7)$
$Pb(1)–O(2^{v}) = 2.498(7)$
$Pb(1)–O(2^{i}) = 2.736(7)$
$Pb(1)–O(4^{vi}) = 2.688(7)$
$Pb(1)–O(5^{vi}) = 2.576(7)$
$Pb(1)–O(6^{vi}) = 2.651(7)$
$Pb(1)–O(7) = 2.651(7)$
$Pb(1)–O(10^{vi}) = 2.667(7)$
$Pb(1)–O(11^{vi}) = 2.503(7)$
$Pb(2)–O(1) = 2.664(7)$
$Pb(2)–O(1^{i}) = 2.664(7)$
$Pb(2)–O(13^{viii}) = 2.843(7)$
$Pb(2)–O(3^{ix}) = 2.843(7)$
$Pb(2)–O(6^{viii}) = 3.137(7)$
$Pb(2)–O(6^{ix}) = 3.137(7)$
$Pb(2)–O(9) = 2.79(1)$
$Pb(2)–O(10^{vi}) = 2.36(1)$

Symmetry codes

i:	x; $\frac{1}{2}-y$; z
ii:	x; $1-y$; $-\frac{1}{2}+z$
iii:	$\frac{1}{2}+x$; y; $\frac{1}{2}-z$
iv:	x; $\frac{3}{2}-y$; z
v:	x; $-\frac{1}{2}+y$; $1-z$
vi:	$\frac{1}{2}-x$; $-\frac{1}{2}+y$; $\frac{1}{2}+z$
vii:	$-x$; $1-y$; $1-z$
viii:	$1-x$; $1-y$; $1-z$
ix:	$1-x$; $-\frac{1}{2}+y$; $1-z$

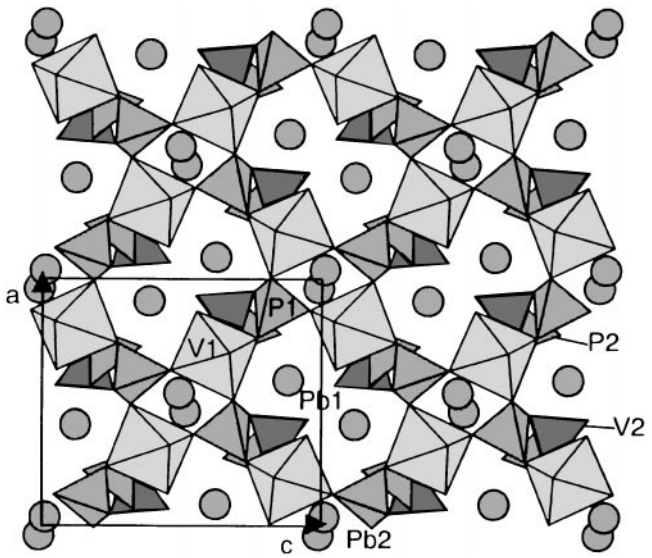

FIG. 4. Projection of the structure of β-$PbVO_2PO_4$ along **b**.

The interatomic distances (Table 3) show that the geometry of the PO_4 tetrahedra is close to that generally observed with P–O bonds ranging from 1.53 to 1.57 Å. The VO_6 octahedra exhibit a geometry very similar to that of α-$PbVO_2PO_4$ with two abnormally short V–O bonds (1.648 and 1.642 Å) corresponding to free apices, two opposite abnormally long V–O bonds (2.210 and 2.139 Å), and two intermediate ones (1.961 and 2.024 Å). In the same way, the VO_4 tetrahedra are characterized by two abnormally short V–O bonds (1.61 and 1.62 Å) corresponding to free apices and two longer ones (1.961 and 2.024 Å). The lead cations exhibit two sorts of coordination, 9-fold for Pb(1) with Pb–O distances ranging from 2.503 to 2.892 Å and 8-fold for Pb(2) with distances ranging from 2.36 to 3.13 Å.

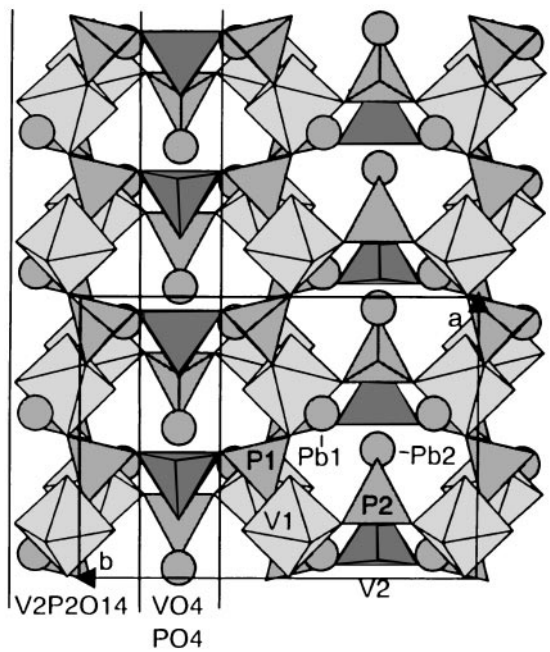

FIG. 5. Projection of the structure of β-$PbVO_2PO_4$ along **c**.

INFRARED STUDY

$PbVO_2PO_4$ α and β phases have also been submitted to spectroscopic analysis together with the isotypic α-$SrVO_2PO_4$ and α-$BaVO_2PO_4$ compounds. FTIR experiment has been performed on a KBr pressed disk containing 2% of the analyzed phase accurately dispersed. The spectra have been recorded by a Nicolet Magna 550 FT-IR spectrometer (resolution 4 cm^{-1}) equipped with a KBr beam splitter and treated by the help of the Nicolet OMNIC software.

The so-obtained spectra are shown in Fig. 7. The band assignment is easier for the α phases (12–15). In the region 1120–1020 cm^{-1} we find the bands due to the asymmetric stretch $\nu_{as}(PO_3)$ of the phosphate groups, followed by the corresponding symmetric mode $\nu_s(PO_3)$ at around 1000 cm^{-1}. In the range 1000–900 cm^{-1} we observe the same components due to the ν(V=O) stretching modes of the vanadyl species, while the strong features at lower wave numbers can be tentatively assigned to the ν_s(VOV) stretch of the nearly square planar V_2O_2 units belonging to the VO_6 edge-sharing octahedra. Between 700 and 570 cm^{-1} we expect the corresponding asymmetric stretch components. In the spectral range below, several bands are present and likely assigned to the δ(OPO) bendings; the symmetric vibrations are placed at the lowest wave numbers.

In general, we observe that the peaks in the $SrVO_2PO_4$ spectrum present a maximum at higher wave numbers with respect to $BaVO_2PO_4$. We can justify this fact by taking into account the average shorter distances in the corresponding V–O and P–O bonds (10), probably due to the slightly greater electronegativity of Sr with respect to Ba. In the $PbVO_2PO_4$ compound, the V–O(1) and P–O(1) bonds are remarkably longer; this affects mainly the $\nu_{as}(PO_3)$ mode of the phosphate tetrahedra undertaking the corresponding band wave numbers to lower values.

The spectrum due to the β-$PbVO_2PO_4$ compound is a little more difficult to be interpreted. Generally speaking, it presents a broad and unresolved absorption massif on which several components are detectable. The maxima are not far from the assignment given above for the α phases. The broadening of the infrared spectrum could be correlated with the crystal structure: in this case all the vanadium and phosphorus polyhedra are connected by corners, having only two free apices for vandium octahedra and tetrahedra. This gives rise to a strong coupling of the vibrations with a consequent loss of resolution.

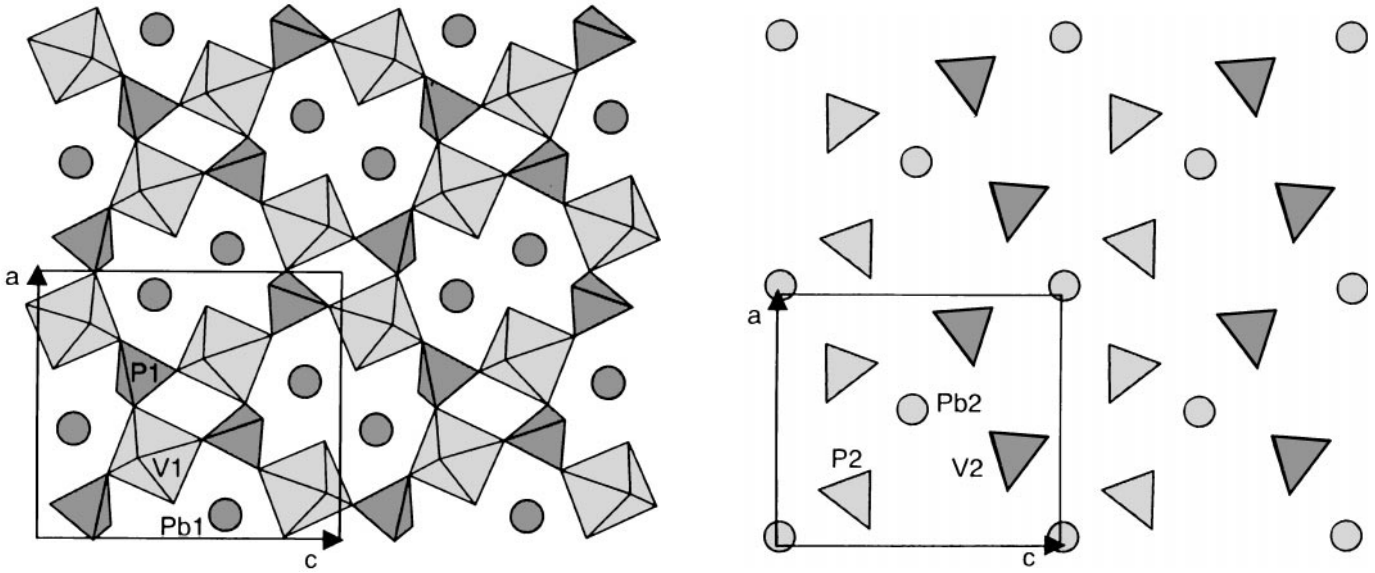

FIG. 6. Projection along **b** of (a) the $[V_2P_2O_{14}]_\infty$ layer and (b) the tetrahedral layer (PO_4 and VO_4).

CONCLUDING REMARKS

This investigation of the V(V) phosphate $PbVO_2PO_4$ shows the existence of two forms, α and β, obtained by hydrothermal synthesis and solid state reaction, respectively. It confirms that the α form is isostructural to the bidimensional Sr and Ba phases previously synthesized (10). In contrast to the latter, the β form exhibits an original tridimensionnal tunnel structure. The study of the transition between the two forms shows that α transforms into β in an irreversible way, by being heated in air above 450°C. Attempts to prepare the β forms of the barium and strontium compounds by solid state reaction were unsuccessful. Finally, it must be emphasized that, in both structures, divalent lead does not show any significant stereoactivity of its $6s^2$ lone pair, in contrast with many Pb(II)-based oxides.

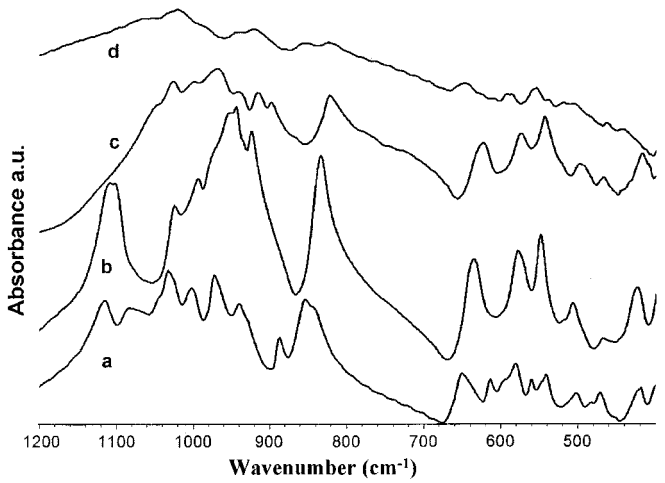

FIG. 7. FTIR spectra of α-$SrVO_2PO_4$ (a), α-$BaVO_2PO_4$ (b), α-$PbVO_2PO_4$ (c), and β-$PbVO_2PO_4$ (d).

REFERENCES

1. G. Centi, F. Trifino, J. R. Ebner, and V. M. Franchetti, *Chem. Rev.* **88,** 55 (1988).
2. B. L. Hodnett, *Catal. Rev.-Sci. Eng.* **27,** 373 (1985).
3. V. C. Kathius, R. D. Hoffmann, J. Huang, and A. W. Sleight, *Chem. Mater.* **5,** 206 (1993).
4. V. C. Kathius, R. D. Hoffmann, J. Huang, and A. W. Sleight, *J. Solid State Chem.* **105,** 294 (1993).
5. H. Y. Kang, S. L. Wang, P. P. Tsai, and K. H. Lii, *J. Chem. Soc., Dalton Trans.* 1525 (1993).
6. F. Berrah, M. M. Borel, A. Leclaire, M. Daturi, and B. Raveau, *J. Solid State Chem.* **145,** 643 (1999).
7. K. L. Idler and C. Calvo, *Can. J. Chem.* **53,** 3665 (1975).
8. J. M. Kiat, P. Garnier, G. Calvarin, and M. Pinot, *J. Solid State Chem.* **103,** 490 (1993).
9. S. Boudin, A. Grandin, A. Leclaire, M. M. Borel, and B. Raveau, *J. Solid State Chem.* **111,** 365 (1994).
10. H. Y. Kang, S. L. Wang, and K. H. Lii, *Acta Crystallogr. C* **48,** 975 (1992).
11. N. E. Brese and M. O'Keeffe, *Acta Crystallogr. B* **47,** 192 (1991).
12. G. Centi, F. Trifirò, G. Busca, J. Ebner, and J. Gleaves, *Discuss. Faraday Soc.* **87,** 215 (1989).
13. G. T. Stranford and R. A. Condrate, *J. Solid State Chem.* **52,** 248 (1984).
14. L. Lezama, J. M. Rojo, J. L. Pizarro, M. I. Arriortua, and T. Rojo, *Solid State Ionics* **63–65,** 657 (1993).
15. J. Kumamoto, *Spectrochim. Acta* **21,** 345 (1965).